# CHAPTER - III

# CHAPTER – III

# PREPARATION OF FERRITE – FERROELECTRIC COMPOSITES AND CHARACTERISATION

## SECTION – A

## PREPARATION OF FERRITE – FERROLECTRIC COMPOSITES

### 3A.1 INTRODUCTION

The materials produced by mixing intimately two or more materials are known as composites. This type of materials fulfils the requirements of engineering. In order to prepare polycrystalline composites some kind of solid state reaction has to take place for developing intimate contact and mixing. The mixture of powders is heated to a high temperature to achieve such a solid state reaction. The reacted material is then ground to a fine powder, which is formed into the required shape and size and again heated to a high temperature to form homogeneous solid. The density, porosity and the microstructure of the sample prepared depend on the method of preparation. The purity of the starting materials, degree of mixing, sintering temperature, sintering time and the microstructural factors such as grain size, defect concentration, pores, grain shape etc. affect the properties of materials thus formed. Therefore during preparation itself various factors are controlled to make better materials or composites [1].

## 3A.2 STANDARD CERAMIC METHOD OF PREPARATION

The most widely used technique is the classical ceramic method. In this method pure metal oxides or the starting constituent phases are chosen. They are thoroughly and uniformly mixed with special techniques. This mixture is sintered for a prolonged time at a fixed temperature in order to attain solid state reaction among the oxides or the constituents and the formation of the compound or the composite.

The ceramic method consists of following stages.

1) Preparation of materials to form an intimate mixture so as to maintain the appropriate proportions of metal ions in the final product.

2) Presintering this mixture to initiate the formation of ferrite, ferroelectric or composite.

3) Powdering the prepared sample and pressing into the required shape to form pellets.

4) Sintering the pressed pellet at elevated temperature.

Generally before one embarks on the ceramic method of preparation of the ferrite the following four methods are used for the preparation of the requisite ferrite compositions.

1) Oxide method

2) Decomposition method

3) Hydroxide precipitation method

4) Oxalate precipitation method

In this first stage itself foundation are laid for the emergence of certain set of properties for the ferrite, ferroelectric or composite especially the microstructure sensitive type.

The second stage of presintering involves heating the intimate mixture of raw materials, in order to decompose carbonates and higher oxides. During this stage solid state reaction takes place and raw materials partly react to produce the final compound. Presintering helps in homogenization, causes partial reaction of the oxides and tends to reduce the shrinkage during the final sintering [2].

The presintered powder is then ground to fine powder so as to reduce particle size and to promote mixing of any unreacted oxides. The dried powder is pressed to required shape using the die and applying pressure of several tonnes from the hydraulic press. The pellets of required shape are thus formed for further processing.

The fourth and the final stage of sintering involve heating the pressed material to high temperature. The sintering involves large-scale diffusion and erasing of the gradients of chemical potentials, resulting in formation of the product, ferrite, ferroelectric or composite. This increases the density and hence reduces the porosity. The final microstructure together with

equilibrium oxygen content and cation distribution depends upon the time and temperature of sintering [3].

## 3A.3 ACTUAL METHOD USED FOR PREPARATION

The ceramic method is easy and economical. Moreover oxides are available with requisite purity of Analytical grade. Hence we have chosen ceramic method for the preparation of ferrite, ferroelectric and the ferrite-ferroelectric composites.

### 3A.3.1 PREPARATION

#### Preparation of Ferrite and Ferroelectric

While preparing ferrite samples by standard ceramic method using A. R. grade oxides, in the present work we have chosen $MnFe_{1.8}$ $Cr_{0.2}O_4$ as it is a magnetostrictive phase. $Mn^{3+}$ and $Cr^{2+}$ are Jahn-Teller ions which cause deformation in the ferrite lattice, that is one of the pre-requisites for composites to exhibit magnetoelectric output (ME output).

$MnFe_{1.8}$ $Cr_{0.2}O_4$ was prepared through normal solid state reaction taking $MnO_2$, $Cr_2O_3$ and $Fe_2O_3$ in molar proportion. These oxides were weighed in required molar proportion using single pan semimicrobalance. The table 3A.1 gives the gives the weights of the oxides taken for the preparation of $MnFe_{1.8}Cr_{0.2}O_4$.

**Table 3A.1**

**Fractional gram molecular weights of powders for $MnFe_{1.8}Cr_{0.2}O_4$ ferrite.**

| Oxides | Weight in grams |
|---|---|
| $MnO_2$ | 10.867 |
| $Cr_2O_3$ | 1.8999 |
| $Fe_2O_3$ | 17.965 |

Similarly ferroelectric phase i.e. $BaTiO_3$ was prepared starting with basic oxides taking $BaCO_3$ and $TiO_2$ in molar proportion. The Table 3A.2 gives the fractional gram molecular weights of starting materials for Barium titanate.

**Table 3A.2**

**Fractional gram molecular weights of powders for $BaTiO_3$ ferroelectric**

| Oxides | Weight in grams |
|---|---|
| $BaCo_3$ | 21.9264 |
| $TiO_2$ | 8.8753 |

The ferrite $MnFe_{1.8}$ $Cr_{0.2}O_4$ and the ferroelectric $BaTiO_3$ were prepared by mixing their basic oxides manually and thoroughly in an agate mortar with acetone as medium. The mixtures were ground to fine powder for a couple of hours.

$MnFe_{1.8}Cr_{0.2}O_4$ and $BaTiO_3$ were presintered at $600^0$ and $800^0$ respectively.

**Preparation of Composites**

Composites with composition $XBaTiO_3$ - (1-X) $MnFe_{1.8}Cr_{0.2}O_4$ with X varies as 0.85, 0.70 and 0.55 in molar percentage were then prepared by mixing $MnFe_{1.8}Cr_{0.2}O_4$ and $BaTiO_3$ thoroughly. The table 3A.3 gives the fractional gram molecular weights of $BaTiO_3$ and $MnFe_{1.8}Cr_{0.2}O_4$ taken to prepare the said composites.

**Table 3A.3**

**Fractional Gram molecular weights of powders for $MnFe_{1.8}Cr_{0.2}O_4$ - $BaTiO_3$ composite.**

| Composition | Weight in grams |
|---|---|
| X=0.85 | 11.635175 |
| X=0.70 | 11.609995 |
| X=0.55 | 11.584815 |

**3A.3.2 Presintering and Grinding**

The composite mixture placed in the platinum crucibles was then presintered at $900^0$ for about 12 hours in air in a globar furnace and then the furnace was cooled slowly. This stage is called presintering of milled composites, is likely to be a final stage of sintering for constituents ferrite and ferroelectric. The temperature of the furnace was measured with the help of chromel alumel thermocouple which was calibrated by usual method. The presintered samples of the composite were ground in an agate mortar for two hours and finally the powder was collected in a clean glass tube.

### 3A.3.3 PELLET FORMATION

To prepare a pellet, a small quantity of powder was ground in acetone by adding few drops of polyvinyl acetate. The powder was poured into a punch die of 1.5 cm diameter and pressed in a hydraulic press with the pressure of the order of 6 to 8 tonnes per square inch for about 5 to 7 minutes. In this way pellets for each sample were prepared.

### 3A.3.4 FINAL SINTERING

The prepared pellets were placed on a thin platinum foil and kept in a globar furnace at a temperature of $1100^0$C for about 12 hours in an air medium for the completion of solid state reaction leading to formation of constituent ferrite and ferroelectric phases as well as to formation of the composite. This was evidenced for the x-ray diffraction patterns. Then the furnace was cooled at the rate of $80^0$ C per hour. Finally the pellets were polished so that opposite faces become exactly parallel to each other. After polishing every pellet was carefully weighed on a microbalance and its dimensions were measured using thickness gauge and physical density was determined.

## SECTION – B

# X-RAY DIFFRACTION STUDIES

### 3B.1 INTRODUCTORY REMARKS ON POWDER METHOD

The X – ray diffraction methods are widely used to characterize the materials, crystals as well as amorphous materials. The powder method was developed by Debye and Scherrer [4] and Hull [5] independently. In this method the crystal to be examined is reduced to a very fine powder and placed in a beam of monochromatic x-rays. Each particle of the powder is a tiny crystal, oriented at random with respect to the incident beam. The result is that every set of lattice planes will be capable of reflection. This method is widely used in the study of ferrite and composite materials. It is very suitable for identification and for determination of the structures of crystals of high symmetry. By using this method the accurate value of lattice parameter can be found out.

### 3B.2 X-RAY DIFFRACTOMETER

The crystal structure analysis can be done by x-rays diffractometer. The schematic diagram of the x-ray diffractometer is shown in fig 3B.

The specimen 'C' is in the form of a fine powder, which is mounted on the table 'H', that is capable of rotating about an axis passing through 'O'. The incident beam of x-rays is allowed to pass through the slit A of the

collimator. As the crystallites are randomly oriented, a reflection of particular position is due to a set of atomic planes, which satisfy Bragg's condition. The diffracted beam gets converged and focused at slit 'F; which further enters the counter 'G', connected to a count rate meter and output of the circuit is fed to a fast automic recorder which registers counts per sec. verses 2ø. The location of the centroid of the recorded peak gives $2ø_{hkl}$ for corresponding Bragg's reflection. The reciprocal lattice lies on the surface of radials (hkl) and is oriented for every possible value of hkl cutting the Ewald's sphere. By Geometry of Ewald's sphere

$$4ø_{hkl} = S_{hkl} / R \qquad \text{.....(1)}$$

If we consider two consecutive reflections, the angle between them is Bragg's angle and is given by

$$ø_{hkl} = S_{hkl} / 4 \qquad \text{.....(2)}$$

Using Bragg's law, we have

$$2d_{hkl} \ Sinø_{hkl} = \lambda \qquad \text{.....(3)}$$

The interplaner spacing $d_{hkl}$ can be determined.

The location of centroid of the recorded peak gives 2ø for corresponding Bragg reflection. However, in modern X-ray diffractometer, proportional or scintillation counter is mounted which records automatically a graph of intensity of x-rays with respect to the Bragg's angle. The main

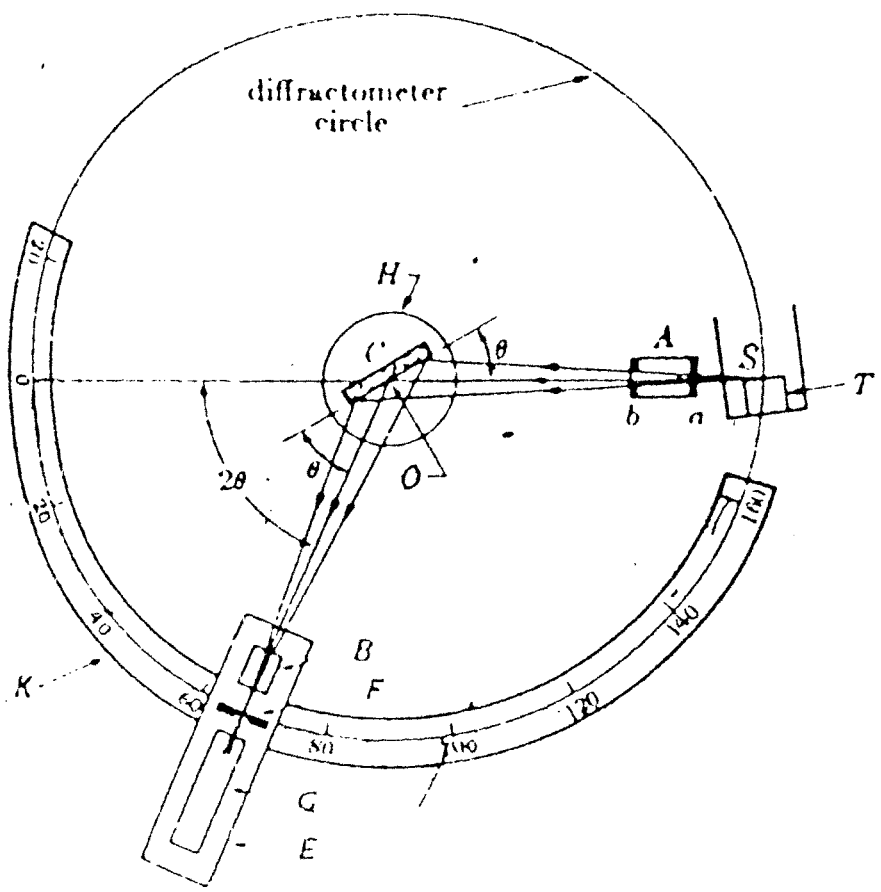


PRINCIPLE OF THE X-RAY DIFFRACTOMETER

advantages of the diffractometer over the debye scherrer camerq is, it gives a quantitative measure of intensity of diffracted beam.

### 3B.3 EXPERIMENTAL TECHNIQUE

The x-ray diffraction patterns of all the samples were taken by using CuK$\alpha$ radiation of wavelength 1.54A$^0$ on Philips PW 1710 diffractometer available at CFC (Common Facility Centre) Shivaji University, Kolhapur. The diffraction maxima occur when the Bragg's condition is satisfied.

The bragg's condition is

$$2d\sin\theta = n\lambda \qquad \ldots\ldots\ldots(4)$$

For a cubic structure interplaner distance 'd', the lattice constant 'a' and the Miller indices 'hkl' of reflecting planes are related by [6, 7]

$$d = a / ( h^2 + k^2 + l^2 )^{1/2} \qquad \ldots\ldots\ldots(5)$$

substituting the value of d from eq$^n$ (5) into equation (4) and rearranging we get

$$a = n\lambda (h^2+k^2+l^2)^{1/2} / 2\sin\theta \qquad \ldots\ldots(6)$$

Using eq$^n$ (6) lattice parameter 'a' can be calculated for the first order. The above equation, after squaring, reduces to

$$[h^2+k^2+l^2] = (4a^2/\lambda^2) \sin^2 \theta \qquad \ldots\ldots\ldots(7)$$

For a particular sample $4a^2/\lambda^2$ is constant. The different peaks correspond to different values of ø, from which the value of $(h^2+k^2+l^2)$ is determined. Using this value the indices hkl of each plane can be determined.

For tetragonal system, the relation between interplaner spacing and lattice constants

$$1/d^2 = (h^2+k^2)/a^2 + l^2/c^2 \quad \text{.....(8)}$$

To find 'a' trace (hko) planes; ones 'a' is calculated 'c' can be derived from other hkl planes[8].

### 3B.4 RESULTS AND DISCUSSION

X-ray diffraction method is used to confirm the formation of ferrite and ferroelectric phases in all the three composites from their x-ray diffractograms. The x-ray diffraction patterns of the ferrite, ferroelectric and their composites are shown in fig. 1 to fig. 5 which show well defined peaks and no unidentified peak is present. The calculated and observed d values are also shown in the table 3B.1 to 3B.5, which determines their structural parameters.

The present XRD of ferroelectric (fig. 1) confirms tetragonal structure in $BaTiO_3$ and the planes that are allowed such as such as (001), (100), (110), (111), (002), (200), (201), (211), (220), (300) and (301) are observed

in this case. The XRD (fig. 2) of ferrite material has confirmed the formation of single phase spinel structure without any expected tetragonal distortion. The observed planes (200), (311), (222), (400), (420), (422), (440), (442) and (533) are allowed for cubic spinel ferrite.

Fig 3 shows XRD of X = 0.85 composite. There is a structural change in the ferroelectric phase in the composite. The tetragonal structure of $BaTiO_3$. is trasnformed in to cubic structure as seen by disappearance of (001,100) and (002, 200) splittings, characteristic of tetragonal $BaTiO_3$. The intensity of the (110) peak in ferroelectric phase remains the same where as highly intense peak (311) of ferrite is very much reduced which is partly due to small percentage and the probable dispersal of tiny particles in the composite.

Fig. 4 shows the XRD of X = 0.70 composite. The figure reveals that the $BaTiO_3$ phase has retained its tetragonal crystal structure in this composite, which is indicated by the splitting ( 002, 200). The intensity of (110) peak of $BaTiO_3$ phase is reduced whereas the intensity of (311) peak of $MnFe_{1.8}Cr_{0.2}O_4$ phase has increased. Moreover the number of ferrite peaks have also increased. In case of X = 0.55 composite the intensity of (110) peak of $BaTiO_3$ is getting further reduced whereas the (311) peak of $MnFe_{1.8}Cr_{0.2}O_4$ is increased. The BaTiO3 shows splitting in diffraction lines for (001) and (002), indicating the tetragonal crystal structure $BaTiO_3$ phase. The numbers of ferrite and ferroelectric are nearly equal as is expected at such a composition.[9,10]

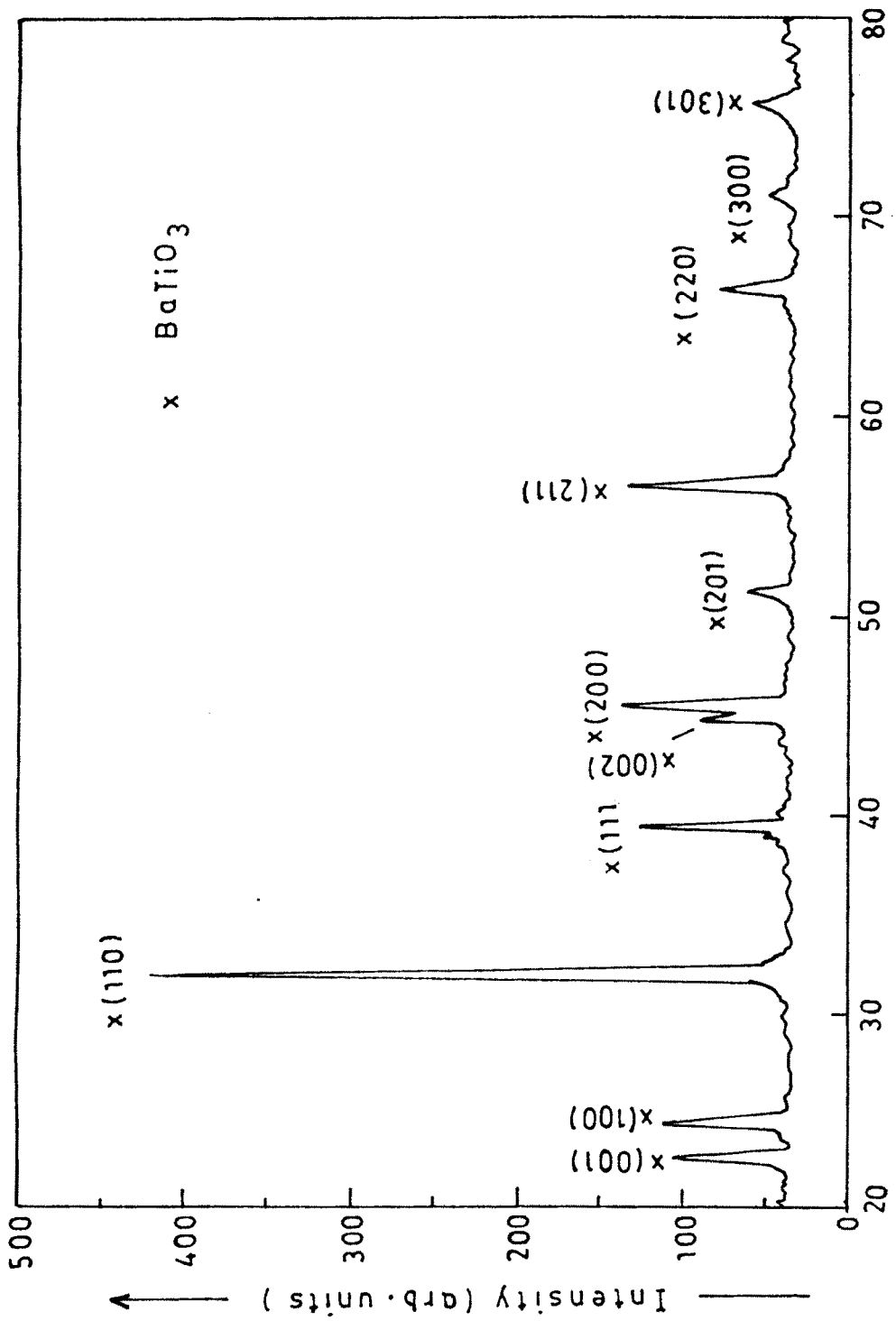


Fig. 1 — XRD of $BaTiO_3$ (Ferroelectric).

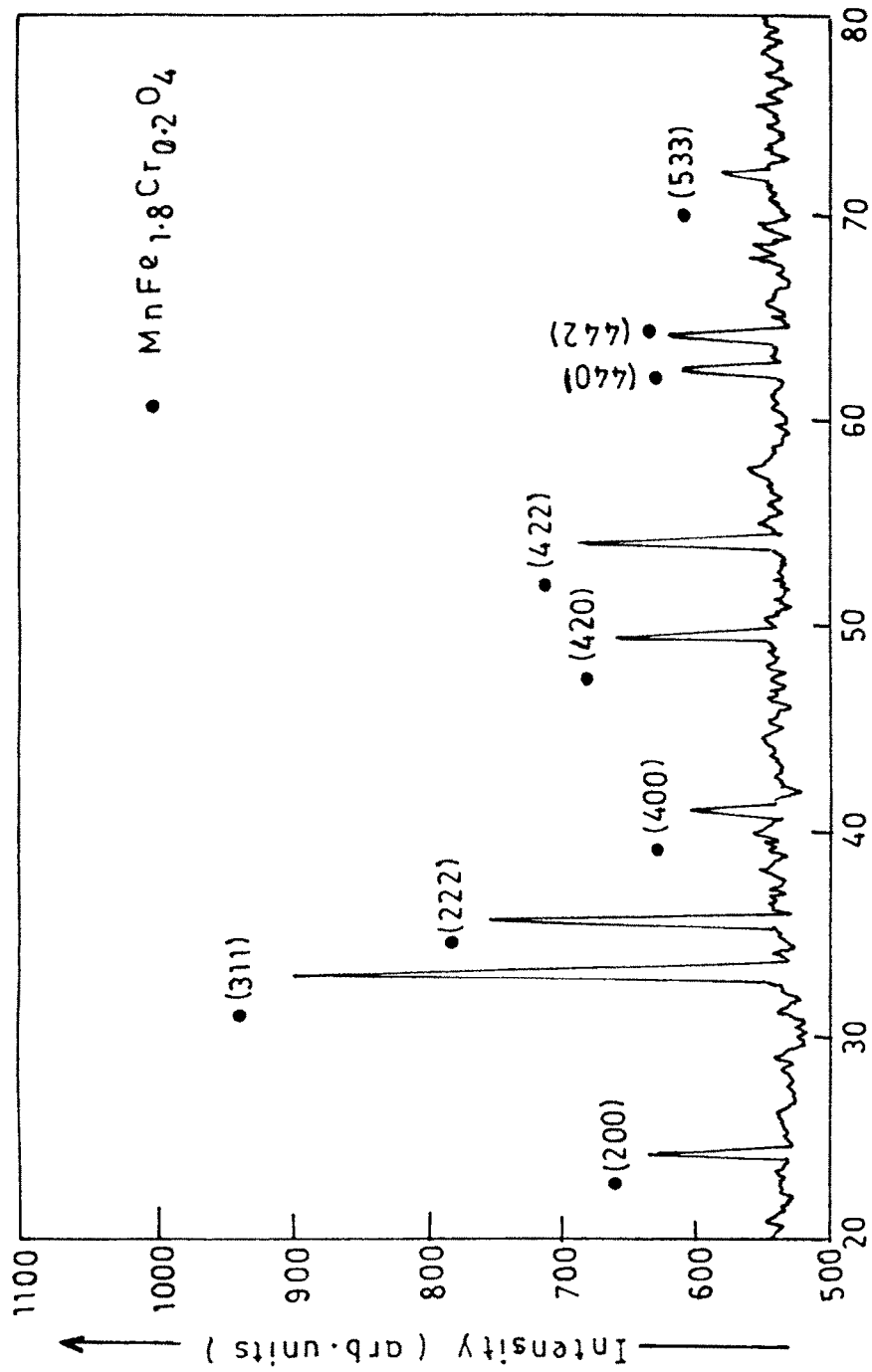


Fig. 2 – XRD of $MnFe_{1.8}Cr_{0.2}O_4$ Ferrite.

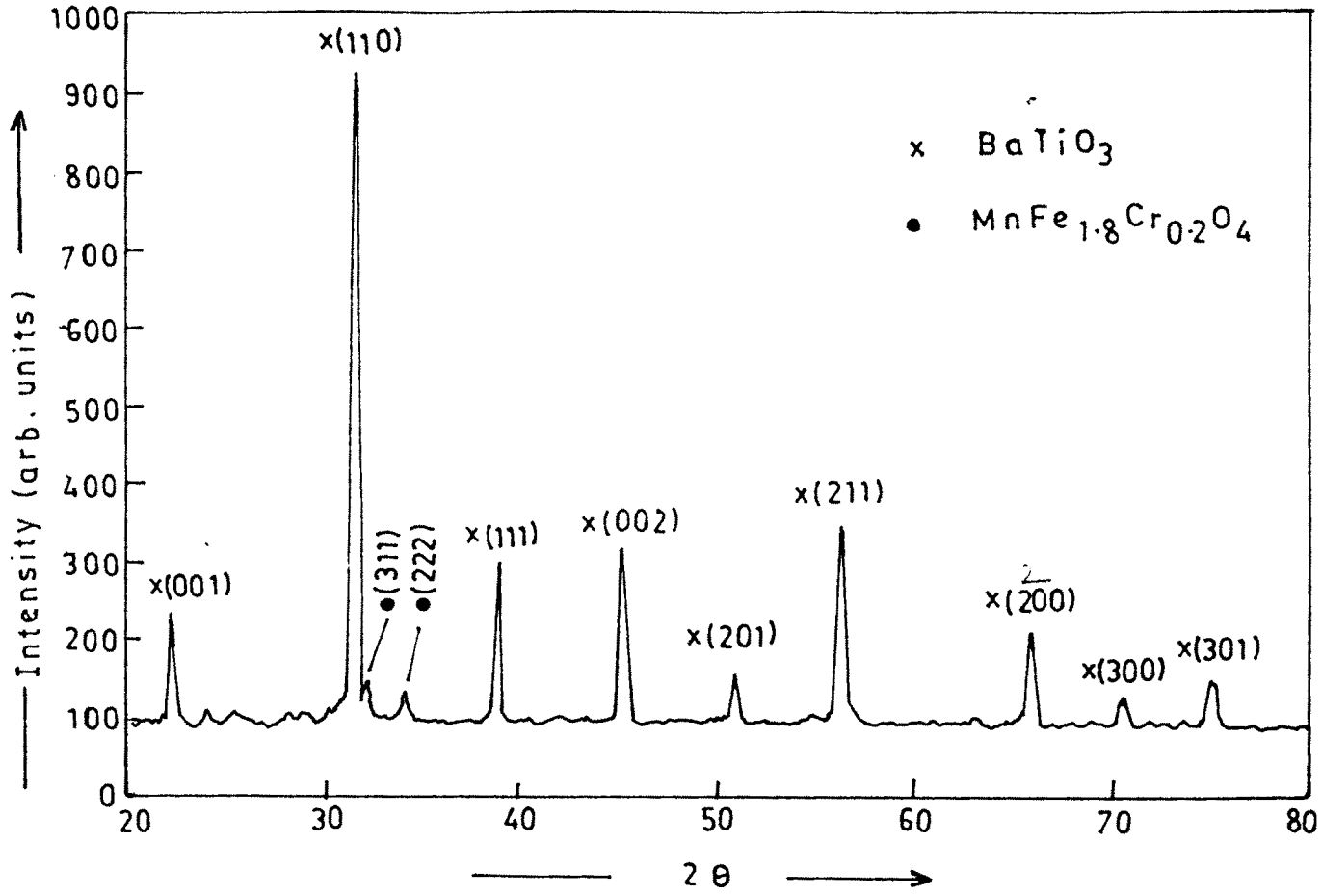


Fig. 3 — XRD Of 85 % $BaTiO_3$ — 15 % $MnFe_{1.8}Cr_{0.2}O_4$ composite.

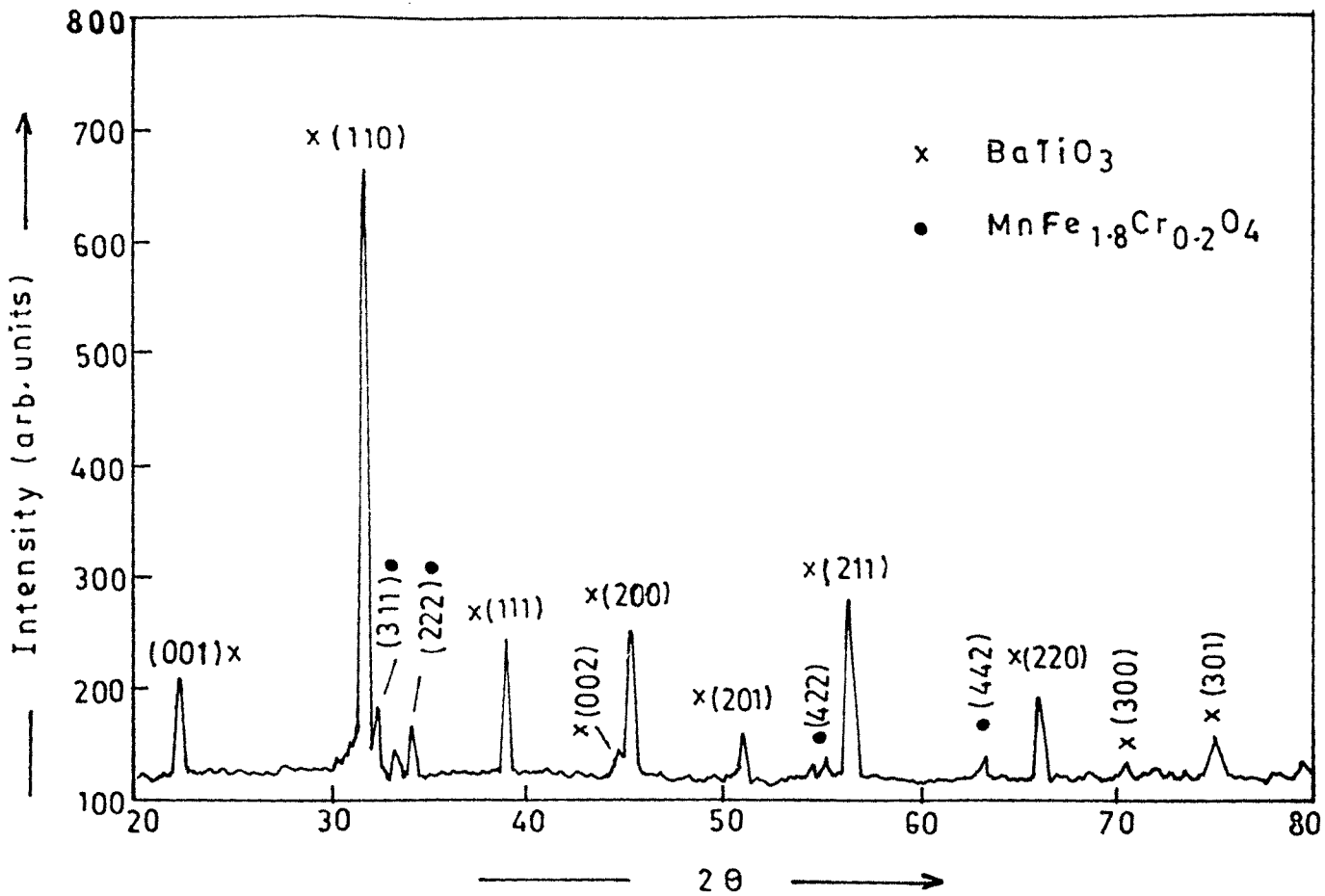


Fig. 4 – XRD of 70 % $BaTiO_3$ – 30 % $MnFe_{1.8}Cr_{0.2}O_4$ .

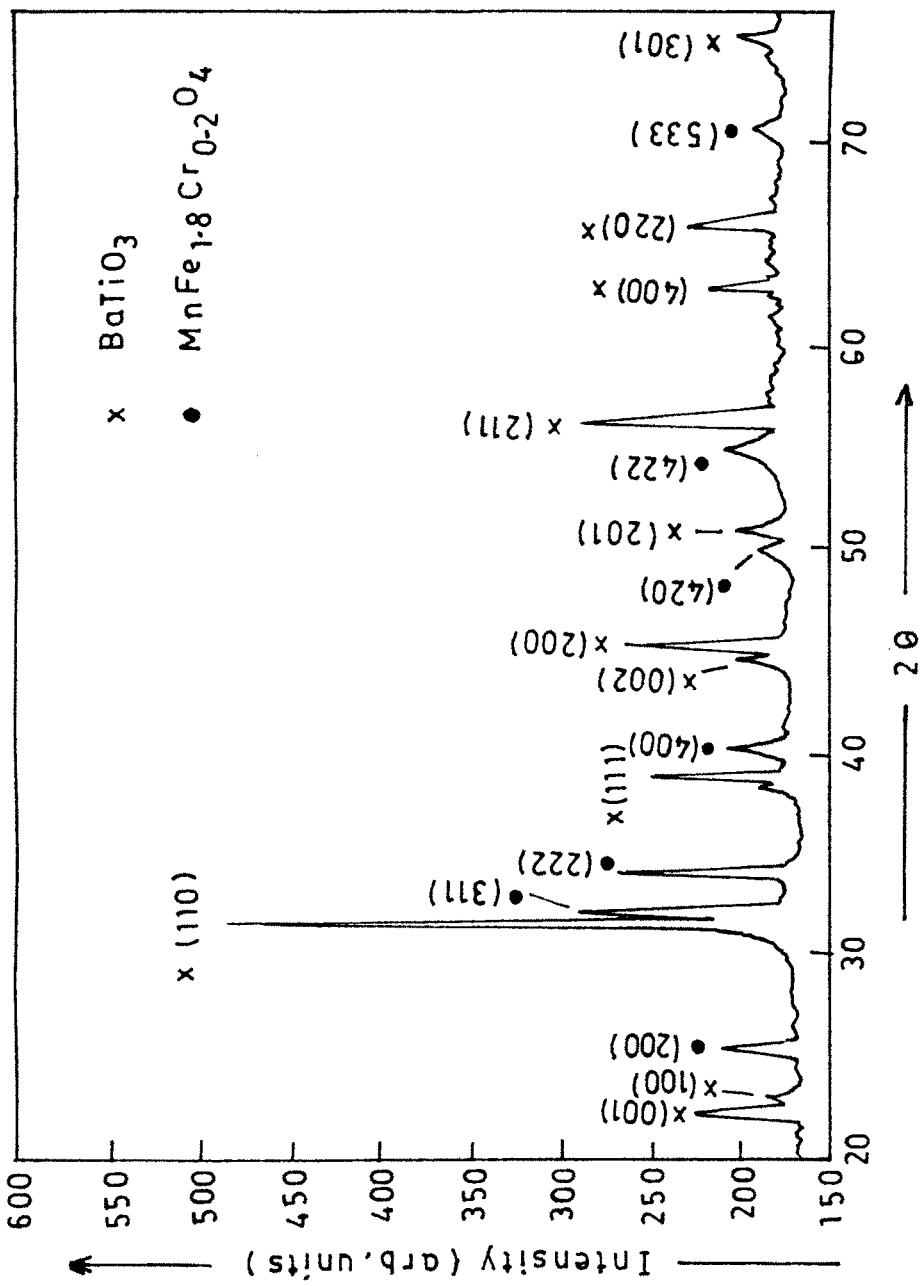


Fig. 5 — XRD of 55% $BaTiO_3$ — 45% $MnFe_{1.8}Cr_{0.2}O_4$.

The calculated and observed d values for indexed planes are in good agreement as seen from tables 3B.1 to .B.5.

**Table 3B.1 : X-Ray Diffraction data of $MnFe_{1.8}Cr_{0.2}O_4$ Lattice parameter a = 8.92935 Å**

| Angle 20 (deg) | dobs (Å) | dcal (Å) | h, k, l |
|---|---|---|---|
| 24.230 | 4.6702 | 4.4645 | 200 |
| 33.250 | 2.6923 | 2.6922 | 311 |
| 35.680 | 2.5143 | 2.5776 | 222 |
| 40.980 | 2.2005 | 2.2323 | 400 |
| 54.175 | 1.6916 | 1.8226 | 422 |
| 62.515 | 1.4845 | 1.5784 | 440 |
| 64.085 | 1.4519 | 1.4882 | 442 |
| 72.150 | 1.3081 | 1.3617 | 533 |

**Table 3B.2 : X-Ray Diffraction Data of $BaTiO_3$ Lattice parameters a = 3.9881 Å c = 4.0372 Å**

| Angle 20 (deg) | dobs (Å) | Dcal (Å) | h, k, l |
|---|---|---|---|
| 22.630 | 3.9260 | 4.0372 | 001 |
| 24.410 | 3.6436 | 3.9810 | 100 |
| 31.945 | 2.7993 | 2.8150 | 110 |
| 39.255 | 2.2932 | 2.3091 | 111 |
| 44.865 | 2.0186 | 2.0186 | 002 |
| 45.535 | 1.9905 | 1.9905 | 200 |
| 51.245 | 1.7813 | 1.7853 | 201 |
| 56.680 | 1.6227 | 1.6290 | 211 |
| 66.375 | 1.4072 | 1.4075 | 220 |
| 71.045 | 1.3258 | 1.3270 | 300 |
| 75.480 | 1.2585 | 1.2606 | 301 |

**Table 3B.3 : X-Ray Diffraction Data of Composite 15% $MnFe^{1.8}Cr_{0.2}O_4$ + 85% $BaTiO_3$**

| Angle 20 (deg) | dobs (Å) | Dcal (Å) | h, k, l |
|---|---|---|---|
| 22.165 | 4.0072 | 4.0372 | 001 |
| 31.545 | 2.8338 | 2.8150 | 110 |
| 32.195 | 2.7850 | 2.6922 | 311 |
| 34.105 | 2.6267 | 2.5776 | 222 |
| 38.895 | 2.3136 | 2.3091 | 111 |
| 45.300 | 2.0052 | 2.0186 | 002 |
| 50.910 | 1.7922 | 1.7853 | 201 |
| 56.195 | 1.6355 | 1.6290 | 211 |
| 65.900 | 1.4162 | 1.4075 | 220 |
| 70.490 | 1.3348 | 1.3270 | 300 |
| 74.810 | 1.2681 | 1.2606 | 301 |

**Table 3B.4 : X-Ray Diffraction Data of Composite 30% $MnFe^{1.8}Cr_{0.2}O_4$ + 70% $BaTiO_3$**

| Angle 20 (deg) | dobs (Å) | Dcal (Å) | h, k, l |
|---|---|---|---|
| 22.305 | 3.9824 | 4.0372 | 001 |
| 31.675 | 2.8225 | 2.8150 | 110 |
| 33.330 | 2.6927 | 2.6922 | 311 |
| 34.185 | 2.6273 | 2.5776 | 222 |
| 39.025 | 2.3061 | 2.3091 | 111 |
| 42.245 | 2.1375 | 2.0186 | 002 |
| 45.410 | 1.9956 | 1.9905 | 200 |
| 51.105 | 1.7858 | 1.7853 | 201 |
| 55.135 | 1.6686 | 1.8226 | 422 |
| 56.135 | 1.6349 | 1.6290 | 211 |
| 62.515 | 1.4882 | 1.4882 | 442 |
| 65.93 | 1.4156 | 1.4075 | 220 |
| 72.150 | 1.3114 | 1.3270 | 300 |
| 75.085 | 1.2641 | 1.2606 | 301 |

**Table 3B.5 : X-Ray Diffraction Data of Composite 45% $MnFe^{1.8}Cr_{0.2}O_4$ + 55% $BaTiO_3$**

| Angle 20 (deg) | dobs (Å) | Dcal (Å) | h, k, l |
|---|---|---|---|
| 22.285 | 3.9859 | 4.0372 | 001 |
| 22.285 | 3.9858 | 3.9810 | 100 |
| 25.495 | 3.4996 | 4.4645 | 200 |
| 31.625 | 2.8268 | 2.8150 | 110 |
| 32.245 | 2.7808 | 2.6922 | 311 |
| 34.105 | 2.6333 | 2.5776 | 222 |
| 37.110 | 2.4206 | 2.3091 | 111 |
| 40.310 | 2.2411 | 2.2323 | 400 |
| 44.615 | 2.0293 | 2.0186 | 002 |
| 45.405 | 1.9958 | 1.9905 | 200 |
| 50.920 | 1.7918 | 1.9966 | 220 |
| 50.920 | 1.7963 | 1.7853 | 201 |
| 54.930 | 1.6743 | 1.8226 | 422 |
| 56.255 | 1.6339 | 1.6290 | 211 |
| 63.040 | 1.4770 | 1.5784 | 440 |
| 65.950 | 1.4188 | 1.4075 | 220 |
| 66.950 | 1.4152 | 1.3617 | 533 |
| 75.050 | 1.2646 | 1.2606 | 301 |

The lattice constants for $BaTiO_3$ , $MnFe_{1.8}Cr_{0.2}O_4$ and their phases in the composites X = 0.85, 0.70 and 0.55 are given in table 3B.6

**Table 3B.6**

**Lattice Constants for Composition**

| Composition | Lattice constants | | | |
|---|---|---|---|---|
| | Ferrite | | Ferroelectric | |
| | a | c | a | c |
| X = 1 | ----- | ----- | 3.981 | 4.0372 |
| X = 0 | 8.98 | ----- | ----- | ----- |
| X = 0.85 | 8.928 | ----- | 4.0075 | 4.0372 |
| X = 0.70 | 8.928 | ----- | 3.980 | 4.0372 |
| X = 0.55 | 8.928 | ----- | 3.980 | 4.0372 |

The lattice parameters of the individual phases in composites remain almost the same. Howerver for X = 0.85 composite the $BaTiO_3$ phase has changed structure from tetragonal to cubic. No explanation for this structural change has been reported by other workers, although similar observations seen to have appeared in these investigations. However this anomaly in structural change observed for X = 0.85 composite can be ascribed to the relative isolation of the constituents of ferrite formation and there effective utilization in affecting the constitution of $BaTiO_3$ structurally.

The porosity for the present samples was determined by liquid immersion technique. Using the formula

$$\% \text{ Porosity} = \rho_x - \rho_a \; / \; \rho_x * 100\%$$

where, $\rho_x$ = x – ray density

$\rho_a$ = actual density/ physical density

The x – ray densities of ferroelectric i.e. $BaTiO_3$ and ferrite $MnFe_{1.8}Cr_{0.2}O_4$ are calculated using the following formulae.

$$\rho_{xBaTiO3} = M / Na^2c$$

where, M = Molecular weight of $BaTiO_3$ expressed in grams.

a & c are lattice constants of $BaTiO_3$

N = Avagadro's number = $6.023*10^{23}$

Similarly x – ray density of ferrite is given by the following formula

$$\rho_{xMnF} = 8M / Na^3$$

where the symbols have the usual meaning.

For the composites the x – ray density is given by

$$\rho_{xcomp.} = M_1 + M_2 / V_1 + V_2$$

where, $M_1$ = X (Mole. Weight of BaTiO3 )

$M_2 = (1 - X)$ (Mole. Weight of MnF)

$V_1 = M_1 / \rho_{xBaTiO3}$

$V_2 = M_2 / \rho_{xMnF}$

Where X assumes values of 0.85, 0.70 and 0.55

Thus the porosities calculated for various compositions are given in table 3B.7. The porosity is minimum for ferrite and maximum for X = 0.85 composite. It is seen from table that the porosities of the composite are larger compared to those of the individual phases, which is likely to be due to postponed formation of the constituents at the final stage of sintering of the composite in order to retain smaller gram sizes of M.E. effect.

**Table 3B.7**

**The Density and Porosity values.**

| Composition (X) | X – ray density $\rho_x$ | Actual density $\rho_a$ | Porosity % |
|---|---|---|---|
| X = 1 | 6.0515 | 5.200 | 14.07 |
| X = 0 | 4.288 | 3.796 | 11.47 |
| X = 0.85 | 5.7039 | 4.523 | 20.70 |
| X = 0.70 | 5.39286 | 4.386 | 18.67 |
| X= 0.55 | 5.1128 | 4.344 | 15.04 |

## REFERENCES


1. Stanley K. J., "Oxide Magnetic Materials", Clarendon Press, New York, Chapt. 2 (1962) 7.

2. Swallo W. D. and Jordon A. K., Proc. Brit. Ceram. Soc. 2 (1964) 1

3. Burke J. E. " Kinetics of high temperature processes", New Y (1959) 109.

4. Debye P. and Scherrer P. Physica, 17 (1916) 277.

5. Hull A. W. Phys. Rev. 9 (1916) 504 and ibid 10 (1917) 661.

6. Henry N.F.M. Lipson H. and Wooster W. A. "Interpretation of X-ray diffraction photographs", McMillan and Co. Ltd., London (1961).

7. Kirichok P. P. and Antoschuk A. I., Acad. Nauk SSSR, Neorganichskic Materials 13 (1977) 1327.

8. Gawade R. J., Ph.D. Thesis, Shivaji University, Kolhapur (1993).

9. K. K. Patankar, S. A. Patil, K. V. Sivakumar, R. P. Mahajan, Y. D. Kolekar, M.B. Kothale Mat. Chem. Phys. , 8667 (2000) (in press)

10. R. P. Mahajan Ph.D. Thesis, Dept of Physics, Shivaji University, Kolhapur. (2000)